MICHIGAN STATE UNIVERSITY

CYCLOTRON LABORATORY

THE $^{34}S(p,t)^{32}S$ REACTION

H. NANN and B.H. WILDENTHAL

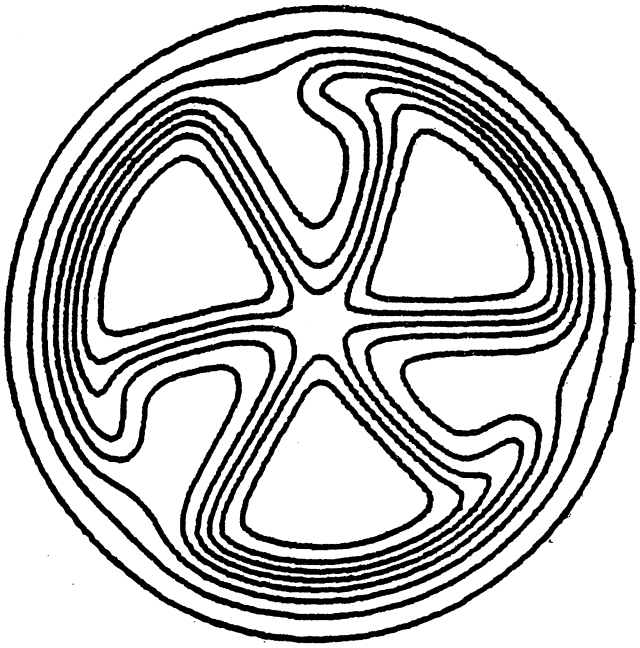

MSUCL-193 OCTOBER 1975

The $^{34}S(p,t)^{32}S$ Reaction*

H. Nann and B.H. Wildenthal

Cyclotron Laboratory and Department of Physics
Michigan State University, East Lansing, Michigan 48824

ABSTRACT

Angular distributions of the $^{34}S(p,t)^{32}S$ reaction at E_p=40 MeV have been measured for states in ^{32}S up to an excitation energy of 11 MeV. Assignments of the L transfers on the basis of the characteristic shapes of the angular distributions yield several new spin and parity assignments for states in ^{32}S. Transitions to several unnatural parity states in ^{32}S were observed with a cross section of about 5 μb/sr. For transitions to the natural parity states distorted-waves analyses based on current shell-model wave functions were performed and compared to the experimental differential cross sections.

[NUCLEAR REACTIONS: $^{34}S(p,t)$, E_p=40 MeV; measured $\sigma(E_t,\theta)$; enriched target. ^{32}S deduced levels, L, J, π.]

*Research supported in part by the U.S. National Science Foundation.

I. INTRODUCTION

In the simplest shell-model, the $2s_{1/2}$ subshell is filled at ^{32}S. The one-particle, one-hole aspects of the ^{32}S level structure can be studied by means of the single-nucleon transfer reactions on the adjacent nuclei ^{31}P and ^{33}S. Since one starts from non-zero spin ground states, the spin values in the final nucleus ^{32}S cannot be determined unambiguously. The two-nucleon transfer reactions on the even target nuclei ^{30}Si and ^{34}S, however, allow unique spin and parity assignments. They also provide information about the two-particle, two-hole character of the ^{32}S levels.

Among the single-nucleon transfer reactions only the $^{31}P(d,n)^{32}S$ [see Ref. 1] and $^{31}P(^3He,d)^{32}S$ [see Ref. 2,3] have been studied. The two-nucleon transfer reaction $^{34}S(p,t)^{32}S$ was used[4] to locate the lowest 0^+, T=2 state in ^{32}S, but no angular distribuitons were measured. In the ^{30}Si $(^3He,n)^{32}S$ reaction only the ground state transition has been studied so far.[5]

The present investigation of the $^{34}S(p,t)^{32}S$ reaction has two aims. One is to extend the present spectroscopic information about the levels of ^{32}S. The assignment of spins and parities to previously unassigned levels furthers the realm of testing nuclear structure calculations simply on the basis of their predicted energy level spectra. The other aim is to test available shell-model wave functions. The comparison of experimental differential cross sections with the results of

microscopic distorted-wave Born approximation (DWBA) calculations based upon matrix elements of the coupled two-particle creation (or annihilation) operator can provide a sensitive test of the wave functions of the initial and final states.

Shell-model wave functions for states of both the target and final nucleus have been calculated by Wildenthal et al.[6,7] Older calculations[6] were carried out by diagonalizing a Hamiltonian consisting of a combination of free and surface delta two-body matrix elements in a truncated $(1d_{5/2})^{n_1}$ $(2s_{1/2})^{n_2}$ $(1d_{3/2})^{n_3}$ basis space with $n_1 \geq 10$. In the following we refer to these wave functions as FPSDI wave functions. In more recent calculations,[7] the constraints on the configuration space were removed and the two-body matrix elements were treated as independent free parameters in an empirically adjustment to best fit experimental ground state binding energies and level spacings. We refer to these wave functions as DSD wave functions.

Spectroscopic amplitudes calculated from these two sets of wave functions were used with DWBA to predict relative cross sections of transitions to states in ^{32}S. The consistency of the ratio of the measured to calculated cross sections then gives measure of the goodness of the theoretical wave functions.

II. EXPERIMENTAL PROCEDURES AND RESULTS

The present experiment was carried out with a 40 MeV proton beam from the Michigan State University cyclotron. The reaction products were detected in a position sensitive wire-counter plastic-scintillator combination on the focal

plane of an Enge split-pole magnetic spectrograph. The target consisted of two layers of enriched ^{34}S (9.6% ^{32}S, 0.4% ^{33}S and 90.0% ^{34}S), sandwiched between layers of Formvar and carbon foils in order to inhibit evaporation during the bombardment. The target thickness obtained was about 140 $\mu g/cm^2$. Throughout the experiment, the target thickness was monitored by continuously recording of the elastically scattered protons from the target material.

Figure 1 shows a composite triton spectrum obtained at $\theta_{lab}=24°$. The whole excitation energy range was covered in two passes, one from 0 to 6 MeV, and the other from 5 to 11 MeV. An overall energy resolution of about 30 keV was obtained. The spectra were analyzed by the peak fitting program AUTOFIT.[8]

Angular distributions were measured from 4° to 55° for transitions to states in ^{32}S up to 10.8 MeV of excitation. They are displayed in Figs. 2-4 and 6-8. Error bars reflect only statistical uncertainties. The absolute cross sections were obtained by normalization to the elastic scattering of protons on ^{34}S obtained between 25° and 50° under identical experimental conditions. The measured elastic scattering cross sections were assumed to have the values calculated in the optical model from the parameters of Becchetti and Greenlees.[9] The accuracy of the absolute cross sections thus determined is estimated to be about $\pm 20\%$.

The excitation energies of the levels observed in the present experiment are given in Table I. Also shown are data from the recent compilation of Endt and van der Leun.[10] Spin

and parity assignments are indicated where they could be made from comparison to the angular distributions of low-lying states with known spin, since the shapes of the angular distributions with the same L value change very little with excitation energy. Values in parentheses indicate less certain assignments.

III. DISCUSSION OF THE RESULTS

A. L=0 transitions

Four levels with excitation energies varying from 0 to 8.51 MeV were observed to be populated by L=0 transitions. They are displayed in Fig. 2. The state at 7.54 MeV in ^{32}S was previously assigned as 0^+ or 1^+ (see Ref. 10). The observed angular distribution eliminates the 1^+ value unambiguously. The transition to the 8.51 MeV state is very weak ($\sigma_{max} \tilde{\approx} 11$ μb/sr), but the key features of an L=0 angular distribution, maxima at 0° and around 25° and minima near 15° and 37°, are still evident.

B. L=2 transitions

Twelve levels are observed to be excited by L=2 angular distributions. They are shown in Fig. 3. In order to identify L=2 angular distributions, a smooth curve characteristic to an L=2 shape was derived from averaging over known experimental L=2 angular distributions. This curve is superimposed in Fig. 3 to the data as a dotted curve. The present 2^+ assignments agree in all cases with those of previous experiments and furthermore in some cases ambiguities have been removed from previous data.

C. L=4 transitions

The angular distributions for four transitions exhibit the characteristic features of L=4 transfer. One additional transition has most probably an L=4 character. The data are displayed in Fig. 4. Here again a characteristic shape has been obtained from experimentally known L=4 angular distributions and drawn as the dotted line through the present data. Figure 5 displays this experimental L=4 shape together with the corresponding L=2 shape. The differences between these two shapes are obvious. The L=2 angular distribution shows a minimum near 32° whereas in the L=4 angular distribution this minimum lies around 44°. The present results yield new assignments of 4^+ to levels at 6.42, 7.97 and 10.28 MeV in ^{32}S.

D. Other transitions

Two natural odd-parity states were excited in the present experiment, the 3^- state at 5.01 MeV and the 1^- state at 5.80 MeV. The angular distributions are displayed in Fig. 6. The transition to the 3^- state is quite strong ($\sigma_{max} \tilde{\approx} 62$ μb/sr), whereas the transition to the 1^- state is very weak ($\sigma_{max} \tilde{\approx} 9$ μb/sr). In the $^{31}P(^3He,d)^{32}S$ reaction[2] the 3^- states at 5.01 MeV is quite strongly excited by $\ell_p=3$ transfer indicating a predominant $[(1d,2s)^{15}\ 1f_{7/2}]$ 1p-1h configuration. The observed (p,t) strength points to some admixture of the type $[(1d,2s)^{16}_{0,0}(1f_{7/2})^2_{0,1}]$ in the ground state wave function of ^{34}S.

Several transitions to known unnatural parity states in ^{32}S are observed with cross sections smaller than 10 μb/sr. Their angular distributions are shown in Fig. 7. The angular distributions of transitions with undefined angular momentum are collected in Fig. 8.

IV. DISTROTED-WAVE ANALYSIS

A. Differential Cross Section Calculations

Microscopic distorted-wave Born approximation (DWBA) calculations were performed using the two-nucleon transfer option of the code DWUCK.[11] In this option the two-particle form factor is calculated by taking into account the individual motions of the two nucleons and projecting out the zero relative angular momentum part according to the method described by Bayman and Kallio.[12] The optical potentials which were used for calculating the distorted waves in the entrance and exit channels were adapted from the literature[13,14] and are given in Table II. The DWBA calculations were normalized according to the procedure of Baer et al.[15] where

$$\left(\frac{d\sigma}{d\Omega}\right)_{exp} = 9.72\ D_o^2 \varepsilon (T_B 1 N_B 1 | T_A N_A)^2\ (2J+1)^{-1} \sigma_{DW}^{LSJ}\ (\theta)$$

The factor D_0^2 is a normalization constant which arises from making the zero-range approximation. The constant 9.72 comes from the choice of the range parameters of the two-body interaction and the size of the outgoing particle in the code DWUCK. The Clebsch-Gordan coefficient accounts for the coupling of the isospin of the residual nucleus T_B to that of the transferred neutron pair to yield the isospin of the target nucleus T_A. The quantity J is the total angular momentum of the transferred neutron pair and σ_{DW}^{LSJ} (θ) is the differenital cross section calculated by the code DWUCK. The factor ε deals with the goodness of the wave function description of initial and final states. A value ε=1 would indicate an ideal wave

function description if the other assumptions such as single-step process were valid.

Spectroscopic amplitudes have been calculated from the two wave function sets described above. The results are presented in Table III for the various final states in ^{32}S. Using these numbers, theoretical differential cross sections were calculated with the code DWUCK. These predicted triton angular distributions are shown as solid lines in Figs. 2-4 in comparison with the experimental data. As shown, each calculated angular distribution is independently normalized for a best fit to the experimental data. From these fits, the quantity ε was determined assuming an empirical normalization factor D_0^2=33 x 10^4 MeV^2 fm^3. The results are listed in Table IV. The correlation between experimental and theoretical levels is based on their excitation energies positions and in a few instances on a comparison of the cross sections.

B. Nuclear Structure Discussion

The extraction of nuclear structure information by DWBA analysis is considerably complicated if two-step processes are present. In a one-step process, as it is described by DWBA, the dominant relative s-state motion of the two neutrons in the outgoing triton ensures that only natural parity states [$\pi=(-)^J$] can be reached in transitions from a 0^+ target. Hence, the observed excitations of the unnatural parity states at 4.70 (1^+), 5.41 (3^+), 6.23 (2^-) and 7.00 (1^+) MeV must proceed through two-step processes. Thus the quantitative aspects of the DWBA analysis for the comparably weak allowed transitions should be taken with caution.

The strength of the ground state transition is underestimated by both the FPSDI and the DSD wave functions. However, the inclusion of about 10% $(1f_{7/2})^2_{0,1}$ pick-up adding constructively to the FPSDI or DSD spectroscopic amplitudes can easily make up for this discrepancy without changing the shape of the angular distribution. As discussed in Sec. III.D. the strong excitation of the 3^- state at 5.01 MeV clearly indicates the existence of $f^2_{7/2}$ components in the ^{34}S ground state wave function. The shape of the angular distribution of the transition to the first excited 0^+ state at 3.78 MeV is not reproduced (see Fig. 2) by either set of wave functions. In this case again, the inclusion of a small amount of $(1f_{7/2})^2_{0,1}$ pick-up, which now interferes destructively with the FPSDI or DSD spectroscopic amplitudes, improves the fits considerably. This is shown in Fig. 9 for the DSD wave functions. The predicted strength, however, is reduced by a factor of 2, thus worsening the value of ε (see Table IV). The L=0 transitions to the 7.54 and 8.51 MeV levels are quite well accounted for by both sets of wave functions, the DSD being slightly favored over the FPSDI wave function.

The magnitudes of the cross sections for the transitions to the first and third 2^+ T=0 states at 2.23 and 5.55 MeV are well reproduced by both the FPSDI and DSD wave functions. The FPSDI wave functions also predict the strengths of the transitions to the second and fourth 2^+, T=0 states at 4.28 and 6.66 MeV correctly, whereas the DSD wave functions underestimate them by factors of 3.8 and 11.7, respectively. Both sets of wave functions reproduce quite well the magnitudes

of the differential cross sections of the transitions to the first and second 2^+, T=1 states. For the third and fourth 2^+, T=1 transitions, the FPSDI wave functions fail quite drastically to predict the strength, whereas the DSD wave functions yield them fairly well.

The shapes of the L=4 angular distributions are quite poorly reproduced at the very forward angles by the DWBA calculations. The transition strengths for the lowest 4^+, T=0 states at 4.46 and 6.42 MeV are in good agreement with the FPSDI and DSD predictions. This good agreement deteriorates for the higher 4^+, T=0 states. The FPSDI wave functions fail to yield the magnitude of the differential cross section for the third and fourth state within a factor of 2. The DSD wave functions account well for the strength of the third 4^+, T=0 transition but underestimate it for the fourth by nearly a factor of 14. The transition strength to the first 4^+, T=1 state at 10.28 MeV is predicted within a factor of 2 by both sets of wave functions.

V. CONCLUSIONS

The $^{34}S(p,t)^{32}S$ reaction has yielded evidence for several new levels in ^{32}S up to an excitation energy of 11 MeV and has established many new spin-parity assignments. Some of the new assignments nicely confirm excitation energy predictions of sd-shell-model calculations, as can be seen from Table IV. The measured differential cross sections are reproduced reasonably well with microscopic distorted-wave Born

approximation (DWBA) calculations which are based on either of two different sets of shell-model wave functions. The essential difference between these two shell-model calculations is a relaxation on the truncation of the configuration space. The present data seem to favor the shell-model calculations which were performed in the full sd basis space, but not in definitive fashion. Some of the discrepancies between observation and the shell-model predictions apparently stem from the omission of the $1f_{7/2}$ orbit in the model space.

The excitation of unnatural parity states in ^{32}S suggests that two-step processes play some role in the reaction mechanism. These processes are not included in the present DWBA calculations. A more detailed quantitative analysis of the present data must therefore await a better understanding of the reaction mechanisms involved.

REFERENCES

1. A.T.G. Ferguson, L. Nilsson and N. Starfelt, Nucl. Phys. A111, 423(1968).
2. A. Graue, L. Herland, J.R. Lien and E.R. Cosman, Nucl. Phys. A120, 513(1968).
3. R.A. Morrison, Nucl. Phys. A140, 97(1970).
4. J.C. Hardy, H. Brunnader and J. Cerny, Phys. Rev. C1, 561(1970).
5. R. Bass, U. Friedland, B. Hubert, H. Nann and A. Reiter, Nucl. Phys. A198, 449(1972).
6. B.H. Wildenthal, J.B. McGrory, E.C. Halbert and H.D. Graber, Phys. Rev. C4, 1708(1971).
7. B.H. Wildenthal and W. Chung, private communication.
8. J.R. Comfort, Argonne National Laboratory (unpublished).
9. F.D. Becchetti and G.W. Greenlees, Phys. Rev. 182, 1190(1969).
10. P.M. Endt and C. van der Leun, Nucl. Phys. A214, 1(1973).
11. P.D. Kunz, Univ. of Colorado (unpublished).
12. B.F. Bayman and A. Kallio, Phys. Rev. 156, 1121(1967).
13. G.W. Greenlees and G.J. Pyle, Phys. Rev. 149, 836(1966).
14. H.P. Morsch and R. Santo, Nucl. Phys. 179, 401(1972).
15. H.W. Baer et al., Ann. Phys. (N.Y.) 76, 437(1973).

Table I. Energy levels of ^{32}S observed in the $^{34}S(p,t)^{32}S$ reaction, compared with previous data.

E_x(MeV) present work	J^π	E_x(MeV) Ref. 10	J^π	$d\sigma/d\Omega$[a] (μb/sr)
0	0^+	0	0^+	2200
2.230	2^+	2.230	2^+	375
3.778	0^+	3.779	0^+	88
4.280	2^+	4.282	2^+	90
4.459	4^+	4.459	4^+	121
4.696		4.695	1^-	4.9
5.007		5.007	3^-	62
5.415		5.413	3^+	4.0
5.553	2^+	5.548	2^+	4.6
5.797		5.798	1^-	8.8
6.230		6.224	2^-	7.5
6.417	4^+	6.410	(1^-4)	32
		6.621	4^-	
6.662	2^+	6.666	$(1,2)^+$	12
6.769		6.762	(2-5)	
6.851	(4^+)	6.852	(2^-4)	5.4
7.000		7.003	1^+;T=1	7.2
7.116	2^+;(T=1)	7.116	2^+;T=1	145
		7.190		
7.349		7.348		
7.415		7.434	$(0-2)^-$	
		7.485	(1-3)	
7.536	0^+;(T=1)	7.535	$(0,1)^+$;(T=1)	160
7.637				
7.702		7.702	$(2-4)^-$	
		7.877	$(0-2)^-$	
7.914				
		7.951	$(2-4)^-$	
7.966	4^+			22
8.121		8.126	1^+;T=1	
8.266				
		8.294	$(2)^-$	
8.336	2^+;(T=1)			57
		8.502	$(0-2)^-$	
8.507	0^+			11.0
		8.694		
8.725				12.0
		8.790		
8.848				
		8.862		

Table I. continued

E_x(MeV) present work	J^π	E_x(MeV) Ref. 10	J^π	$d\sigma/d\Omega$[a] (μb/sr)
9.025		9.022	$(2-4)^-$	15.0
		9.061	$(0-2)^-$	
9.196	2^+;(T=1)			42
		9.207	1^+;T=1	
		9.238	1^-	
		9.290	1^-	
		9.389	2^+	
9.468		9.464	2^+	5.7
		9.486	1^-	
9.650	2^+;(T=1)	9.650	2^+	14.5
		9.660	1^+	
9.704		9.711	2^+	9.1
		...		
9.820		9.817	$(2^+,3^-)$	18.5
9.920	2^+	9.919		29
		...		
10.276	4^+;(T=1)			28
10.370	2^+	10.371	2^+	60
		...		
10.530				
		...		
10.780	2^+	10.779	$(1^-,2^+)$	41
		...		
10.823	2^+	10.827	$(1^-,2^+)$	84

The excitation energies have an estimated uncertainty of ±5 keV for levels up to 8 MeV of excitation and ±8 keV for higher excited states. The assignment of the isospin quantum number T=1 is made on a comparison of the excited ^{32}S spectrum with that of ^{32}P.

a) All cross sections are taken at the maximum in the angular distribution.

Table III. Spectroscopic amplitudes for $^{34}S + A=32$

J_f^π	T_f	E_x(MeV)	J	T		(D5,D5)	(S1,S1)	(D3,D3)	(D5,S1)	(D5,D3)	(S1,D3)
0^+	0	0.00	0	1	a)	+0.2159	+0.3140	+0.8541			
		0.00			b)	+0.4326	+0.2875	+0.7437			
		3.68			a)	-0.0316	-0.3487	+0.2180			
		3.84			b)	+0.0456	-0.3228	+0.3123			
		7.35			a)	+0.2468	+0.0657	-0.0726			
		7.12			b)	-0.0827	+0.1085	+0.1971			
		7.99			a)	+0.0913	-0.1711	-0.0681			
		7.19			b)	+0.2370	-0.1435	-0.1022			
2^+	0	2.20	2	1	a)	+0.1268		+0.1824	+0.2002	+0.0228	+0.8034
		2.40			b)	-0.2670		-0.0422	-0.4791	-0.2710	-0.6465
		4.55			a)	-0.1718		+0.0636	-0.4106	-0.5739	+0.0339
		4.17			b)	+0.1050		-0.3144	+0.3248	+0.3635	-0.1583
		5.44			a)	+0.0697		+0.6962	+0.0057	-0.0068	+0.3856
		5.46			b)	-0.1316		-0.5627	-0.1064	-0.2384	+0.3930
		6.64			a)	-0.1613		+0.1731	-0.5548	+0.4848	+0.2884
		6.95			b)	-0.1301		-0.0568	+0.4046	-0.5588	-0.1587
4^+	0	4.92	4	1	a)	-0.1472				-0.9167	
		4.82			b)	+0.2996				+0.9889	
		5.60			a)	-0.0452				-0.5450	
		6.65			b)	-0.1645				-0.7011	
		6.15			a)	-0.1338				-0.0139	
		7.55			b)	-0.1477				-0.1578	

Table II. Optical potential parameters used in the DWBA calculations.

	V (MeV)	W_v (MeV)	W_s (MeV)	r_o (fm)	a (fm)	r' (fm)	a' (fm)	r_c (fm)
p	47.5		13.0	1.25	0.70	1.25	0.70	1.25
t	173.9	20.6		1.15	0.72	1.50	0.82	1.40

Table IV. $^{34}S(p,t)^{32}S$. Comparison of experimental transition strengths with microscopic DWBA predictions (see text).

J_f^π	T_f	E_x(MeV) Exp.	E_x(MeV) FPSDI	E_x(MeV) DSD	ϵ FPSDI	ϵ DSD
0^+	0	0	0	0	1.91	1.60
2^+	0	2.23	2.20	2.40	1.38	0.81
0^+	0	3.78	3.68	3.84	0.89	2.34
2^+	0	4.28	4.55	4.17	0.81	3.83
4^+	0	4.46	4.92	4.82	1.11	0.81
2^+	0	5.55	5.44	5.46	1.06	1.50
4^+	0	6.42	5.60	6.65	1.06	0.53
2^+	0	6.66	6.64	6.95	0.68	11.7
(4^+)	0	6.85	6.15	7.55	8.94	1.28
2^+	1	7.12	6.71	7.29	1.17	0.89
0^+	(1)	7.54	6.95	7.24	0.55	0.64
4^+	0	7.97	7.52	7.94	23.4	13.8
2^+	(1)	8.34	7.70	8.07	0.62	0.85
0^+	0	8.51	7.35	7.12	0.85	0.81
2^+	(1)	9.20	8.78	9.08	9.79	0.55
2^+	(1)	9.65	9.18	9.77	0.08	2.02
4^+	(1)	10.28	9.42	10.08	0.60	1.92

Table III. Continued.

J_f^π	T_f	E_x(MeV)	J	T		(D5,D5)	(S1,S1)	(D3,D3)	(D5,S1)	(D5,D3)	(S1,D3)
		7.52			a)	+0.0853				-0.1469	
		7.94			b)	+0.1606				+0.0379	
0^+	1	6.95	0	1	a)	-0.2776	-0.6944	-0.0256			
		7.24			b)	+0.2965	+0.6132	+0.0181			
2^+	1	6.71	2	1	a)	-0.1124		-0.2808	-0.0064	+0.2989	-1.2350
		7.29			b)	+0.1384		+0.0315	+0.0919	-0.1711	+1.2486
		7.70			a)	-0.2081		-0.9212	-0.4881	-0.2839	+0.0738
		8.07			b)	+0.2241		+0.9074	+0.3891	+0.0058	-0.0096
		8.78			a)	+0.0612		-0.1464	+0.3220	+0.1418	-0.1300
		9.08			b)	+0.2361		-0.1974	+0.9432	-0.6328	-0.0192
		9.18			a)	-0.3703		+0.1102	-0.9731	+0.1356	-0.3605
		9.77			b)	+0.0724		-0.2800	+0.4090	+0.2088	-0.2625
4^+	1	9.42	4	1	a)	+0.3625				+0.8535	
		10.08			b)	-0.3226				-0.3854	

a) FPSDI wave functions (See Ref. 6)

b) DSD wave functions (see Ref. 7)

FIGURE CAPTIONS

Fig. 1--Composite triton spectrum from the $^{34}S(p,t)^{32}S$ reaction.

Fig. 2--Angular distributions of L=0 transitions observed in the $^{34}S(p,t)^{32}S$ reaction.

Fig. 3--Angular distributions of L=2 transitions observed in the $^{34}S(p,t)^{32}S$ reaction.

Fig. 4--Angular distributions of L=4 transitions observed in the $^{34}S(p,t)^{32}S$ reaction.

Fig. 5--Experimentally obtained shapes for L=2 and L=4 angular distributions.

Fig. 6--Angular distributions of transitions to natural odd-parity states.

Fig. 7--Angular distributions of transitions to unnatural parity states.

Fig. 8--Angular distributions of transitions with undefined transferred orbital angular momentum.

Fig. 9--Influence of small $(f_{7/2})^2_{0,1}$ admixtures to the DSD spectroscopic amplitudes on the shapes of the L=0 angular distributions to the ground and 3.78 MeV states. For the ground state transition only the full line is shown since the $(f_{7/2})^2_{0,1}$ admixtures result in no significantly different angular distributions.

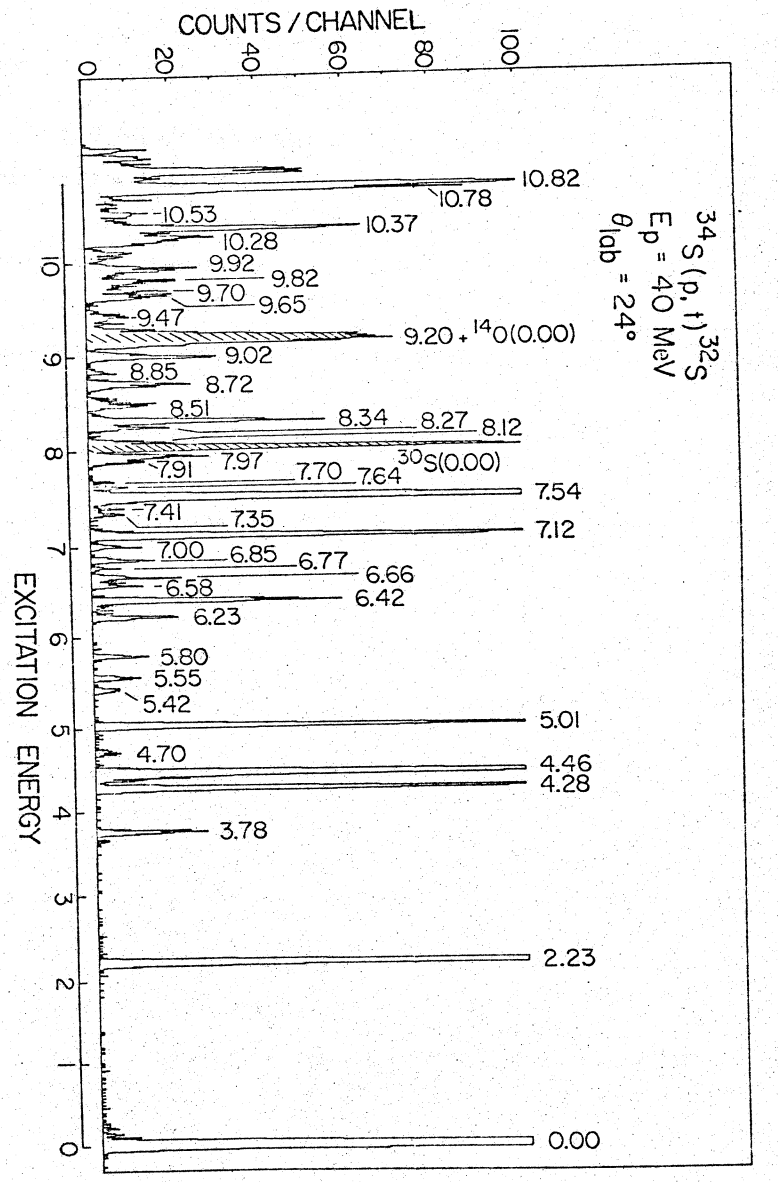

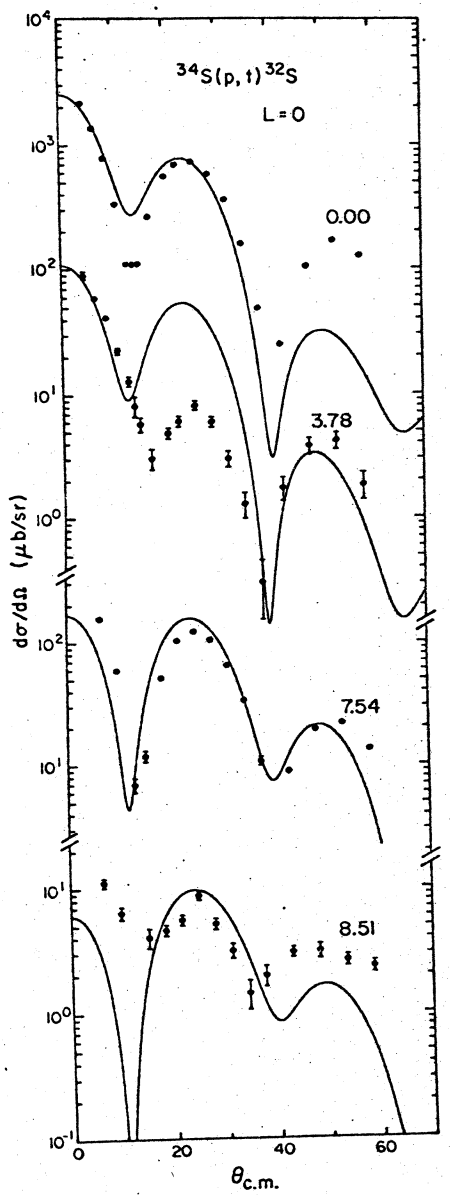
$^{34}S(p,t)^{32}S$
L=0
0.00
3.78
7.54
8.51
$d\sigma/d\Omega$ (μb/sr)
$\theta_{c.m.}$

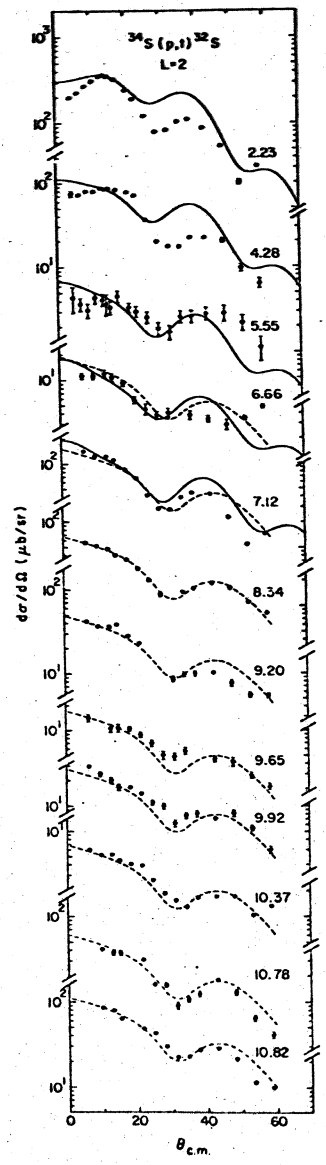
$^{34}S(p,t)^{32}S$
L=2
2.23
4.28
5.55
6.66
7.12
8.34
9.20
9.65
9.92
10.37
10.78
10.82
$d\sigma/d\Omega$ (μb/sr)
$\theta_{c.m.}$

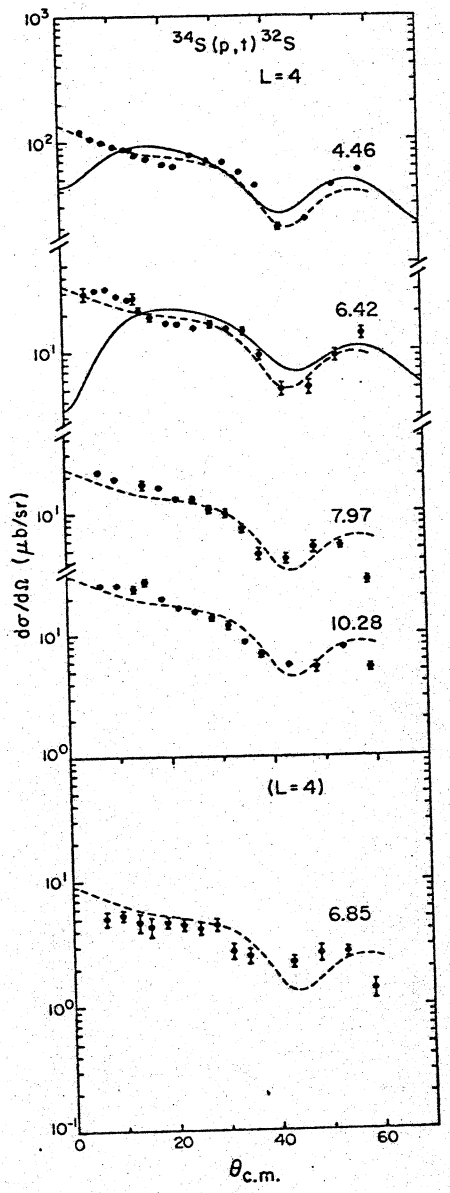
$^{34}S(p,t)^{32}S$
L=4
4.46
6.42
7.97
10.28
(L=4)
6.85
dσ/dΩ (μb/sr)
θc.m.

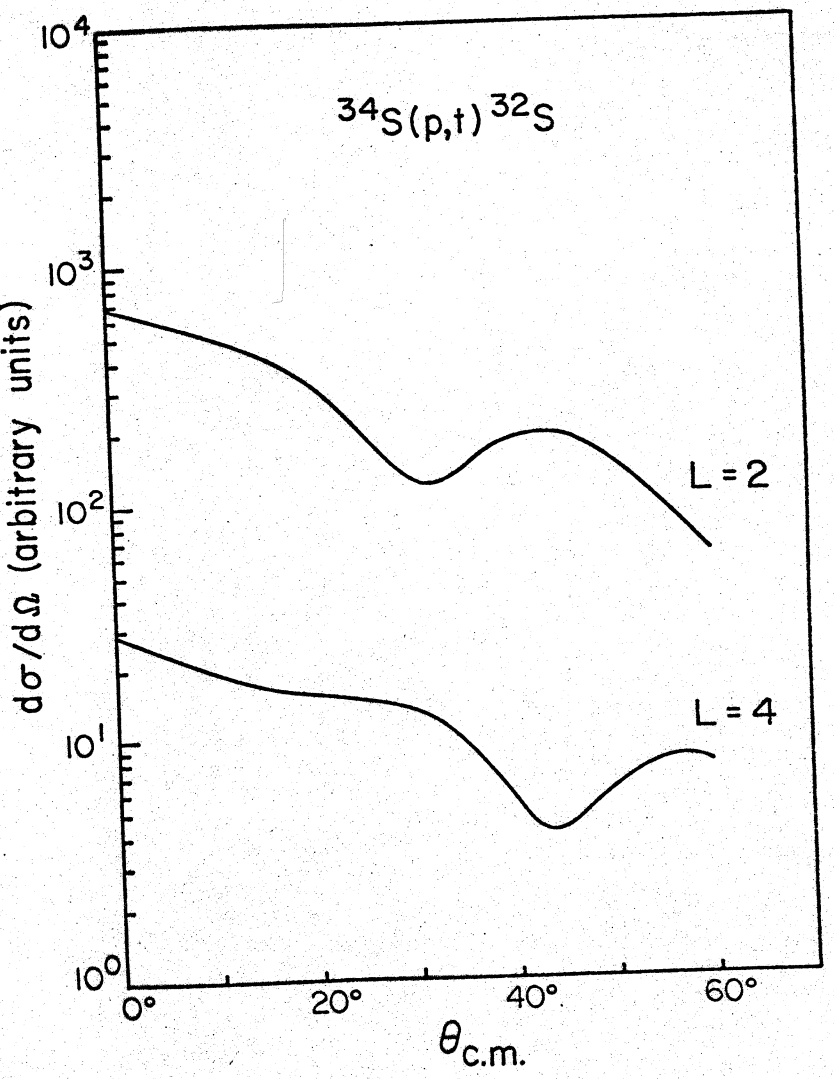
$^{34}S(p,t)^{32}S$
L=2
L=4
dσ/dΩ (arbitrary units)
θc.m.

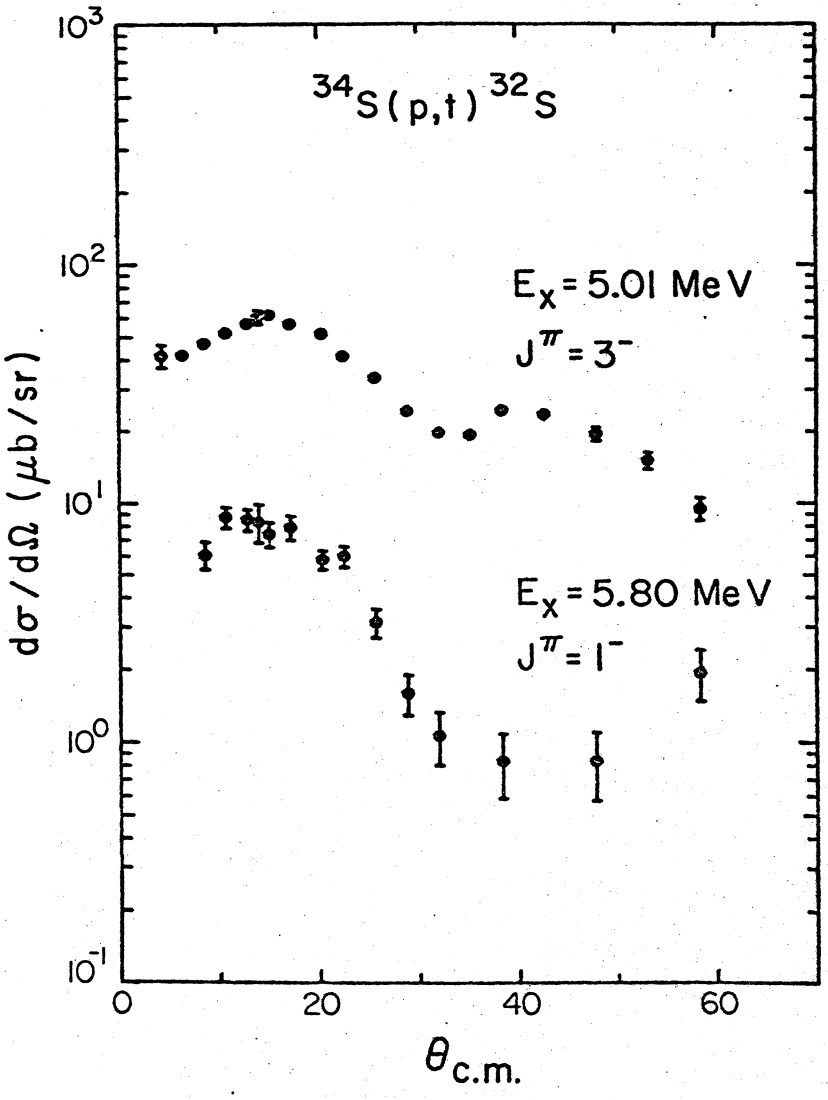
$^{34}S(p,t)^{32}S$
$E_x = 5.01$ MeV
$J^\pi = 3^-$
$E_x = 5.80$ MeV
$J^\pi = 1^-$
$d\sigma/d\Omega$ (μb/sr)
$\theta_{c.m.}$

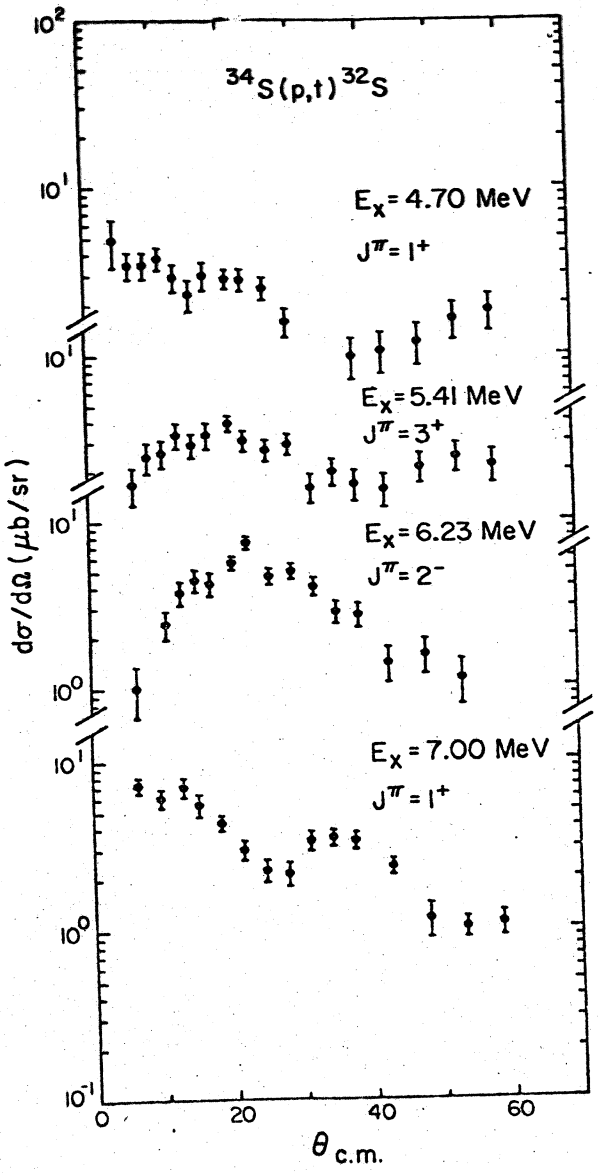
$^{34}S(p,t)^{32}S$
$E_x = 4.70$ MeV
$J^\pi = 1^+$
$E_x = 5.41$ MeV
$J^\pi = 3^+$
$E_x = 6.23$ MeV
$J^\pi = 2^-$
$E_x = 7.00$ MeV
$J^\pi = 1^+$
$d\sigma/d\Omega$ (μb/sr)
$\theta_{c.m.}$

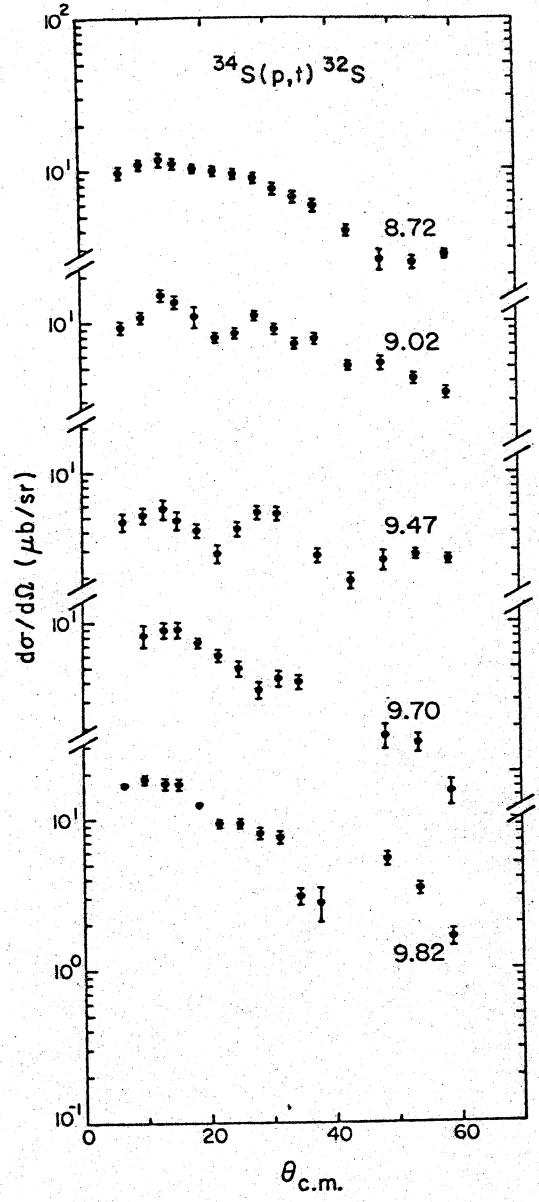
$^{34}S(p,t)^{32}S$
8.72
9.02
9.47
9.70
9.82
$d\sigma/d\Omega$ (μb/sr)
$\theta_{c.m.}$
0
20
40
60

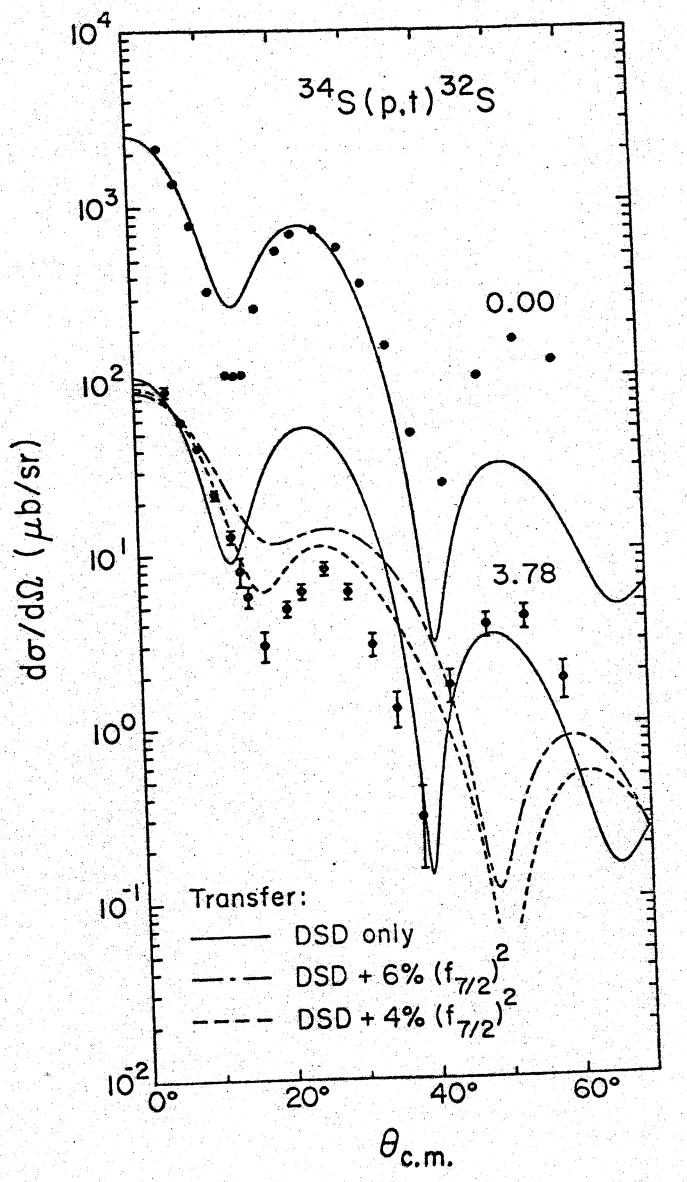
$^{34}S(p,t)^{32}S$
0.00
3.78
Transfer:
DSD only
DSD + 6% $(f_{7/2})^2$
DSD + 4% $(f_{7/2})^2$
$d\sigma/d\Omega$ (μb/sr)
$\theta_{c.m.}$
0°
20°
40°
60°